Radiation Protection Dosimetry (2017), Vol. 176, No. 1-2, pp. 10–31 doi:10.1093/rpd/ncx014
Advance Access publication 16 February 2017

THE MAYAK WORKER DOSIMETRY SYSTEM (MWDS-2013) FOR INTERNALLY DEPOSITED PLUTONIUM: AN OVERVIEW

A. Birchall[1,*], V. Vostrotin[2], M. Puncher[3], A. Efimov[2], M.-D. Dorrian[3], A. Sokolova[2], B. Napier[4], K. Suslova[2], S. Miller[5], A. Zhdanov[2], D. J. Strom[4], R. Scherpelz[4] and A. Schadilov[2]
[1]Global Dosimetry Ltd., 1 Macdonald Close, Didcot, Oxon OX11 7BH, UK
[2]Southern Urals Biophysics Institute (SUBI), Ozersk, Chelyabinsk Region, Russia
[3]Public Health England (PHE), Chilton, Didcot, UK
[4]Pacific Northwest National Laboratory (PNNL), Richland, WA, USA
[5]University of Utah, Salt Lake City, UT, USA

*Corresponding author: GlobalDosimetry@gmail.com

The Mayak Worker Dosimetry System (MWDS-2013) is a system for interpreting measurement data from Mayak workers from both internal and external sources. This paper is concerned with the calculation of annual organ doses for Mayak workers exposed to plutonium aerosols, where the measurement data consists mainly of activity of plutonium in urine samples. The system utilises the latest biokinetic and dosimetric models, and unlike its predecessors, takes explicit account of uncertainties in both the measurement data and model parameters. The aim of this paper is to describe the complete MWDS-2013 system (including model parameter values and their uncertainties) and the methodology used (including all the relevant equations) and the assumptions made. Where necessary, Supplementary papers which justify specific assumptions are cited.

INTRODUCTION

Aim

As part of an ongoing study (Joint Coordinating Council on Radiation Effects Research (JCCRER) Project 2.4), funded by the United States Department of Energy (USDOE), various protocols for assessing the internal doses of Mayak Production Association (PA) workers have been generated: DOSES-1995, DOSES-2000, DOSES-2005 and MWDS-2008. These doses are used as inputs to epidemiological studies (JCCRER Project 2.1) to determine the risk of exposure to plutonium aerosols. The purpose of this paper is to present the latest Mayak Worker Dosimetry System MWDS-2013 in sufficient detail for an independent source to duplicate the doses or scrutinise the methodology. The paper is concerned with internal doses from inhaled plutonium only; external doses are considered in a separate paper. The paper only deals with a subset (~8 000) of the full Mayak Worker Cohort, namely, those workers who have actual measurements (mainly urine). For many workers, the number of urine measurements is small: 40% of the cohort having three or less measurements, 70% less than 9 and only 5% having more than 20 measurements. The paper thus acts both as a template for internal dose reconstruction and a statement for the record as to how the doses are derived. Reference to other papers in this special edition will be made to give more detail and to justify the choice of parameter values made with a scientific basis.

Strategy for dose calculations

In previous studies, a relatively simple biokinetic model was used to define the exact biokinetic behaviour of plutonium following inhalation. The magnitude of the intake can then be inferred by comparing the predicted urinary excretion rates with those measured in practice. This unique intake is, in turn, used together with dosimetric assumptions to determine organ doses for each worker in the cohort.

In this study, there are many differences between the model structures and methodology employed previously, e.g. treatment of dissolution, inclusion of a bound fraction, more up-to-date treatment of particle transport, simplified intake regime based on air sample measurements, treatment of measurement uncertainty, new method of dealing with measurements following Diethylene Triamine Pentaacetic Acid (DTPA), treatment of data less than the limit of detection, use of a deposition model and a new Bayesian fitting methodology. However, the main difference is that this study takes explicit account of uncertainties in model parameters. Previous studies used models which have a single value for each of the model parameters. In this study, probability distributions are specified for important parameters which reflect the uncertainty in that parameter value. To distinguish this type of model from the more usual type of model, they are referred to in this and the accompanying papers as hyper-models. The

output of a hyper-model is thus a distribution of a quantity rather than a single value.

The calculation of the output from a given hyper-model (e.g. organ dose) is relatively straight forward to calculate. One simply chooses a random value for each parameter from its specified distribution and runs the model forward to obtain a unique dose. Repetition of this process will lead to the generation of a distribution of the required output. To use a hyper-model to fit values of a parameter to a given data set is more complicated and requires use of Bayesian techniques. These techniques can be time consuming, and specific methods have been devised which can decrease computation times under certain circumstances[1, 2]. Within the Bayesian methodology, the initial distributions assigned to the parameters in the absence of data are referred to as prior distributions, and the resulting parameter distribution (taking into account the measurement data) are known as posterior distributions.

Table 1 summarises the types of prior parameter distribution that are used in MWDS-2013. The justification for the choice of distributions is contained in Supplementary papers within this special edition.

In addition to the distribution of each parameter, a typical representative value will also be chosen. The purpose of the representative value is 3-fold (*a*) to quality assure software algorithms for solving models, and (*b*) to obtain representative values of doses for comparison with previous estimates and (*c*) for comparison with more conventional biokinetic models (e.g. International Council on Radiation Protection (ICRP) models).

The input to the dose calculation typically consists of measurements of plutonium activity in urine samples donated by workers. In the Mayak cohort, there are also around 500 cases for which autopsy data as well as urine measurements are also available. The output for each worker consists of a series of organ doses delivered in each calendar year. For each organ, in a given year, the set of doses for every member of the cohort is referred to as a realisation. In our case, since we use a hyper-model, the organ dose is not a single value, but a probability distribution of organ dose for that individual, and so to avoid confusion, this is referred to as a hyper-realisation. In all, the output for MWDS-2013 consists of 1000 hyper-realisations (for each organ and for each calendar year).

If a parameter value is unknown, but is the same for each worker, then it is referred to as shared. An example of shared parameters is absorption rates from the lungs to blood, where it is assumed that the rate depends on the chemical form of the material only. Conversely, if a parameter value is unknown, and different for each worker, it is referred to as unshared. An example of this is particle transport within the respiratory tract, which is known to vary between individuals, but is independent of chemical form. Within each hyper-realisation, shared parameters take on the same value, whereas unshared parameters are randomly chosen. The set of hyper-realisations thus preserves the information of shared and unshared parameters.

Thus, for each parameter, the following were derived:

- the prior probability distribution for that parameter (Table 1)
- whether it is ‘shared’ or ‘unshared’ between workers
- a representative/default value for the parameter

However, for the purposes of epidemiological analysis, in order to make risk calculations tractable, the hyper-realisations are currently reduced to representative realisations[3].

Implementation of dose calculations

All of the computer code used to implement the dose calculations was developed independently by both SUBI (Southern Urals Biophysical Institute) and PHE (Public Health England). The SUBI code, PANDORA, was developed from previous code for calculating Mayak PA worker doses. The PHE code, IMBA Professional Plus[4–6], was also extended to implement the MWDS-2013 models described here. Both codes were used as part of an extensive quality assurance procedure described in this issue[7, 8]. A full description of how to deal with uncertainty in the model parameters using a multiple hyper-realisation method[9] and how the hyper-realisations are reduced to realisations[3] are described in other articles in this issue.

Table 1. Parameter definitions for distributions given in tables.

Distribution	*a*	*b*	*c*
Lognormal	Median	Geometric standard deviation	—
Left/right truncated lognormal	Median	Geometric standard deviation	Truncation value
Triangular	Minimum	Maximum	Mode
Uniform	Minimum	Maximum	—
Log-uniform	Minimum	Maximum	—

Structure of this paper

The calculation of organ doses from measurements of activity in urine (and occasionally from autopsy samples for Mayak workers) involves four distinct steps.

- Step 1: Values for the activity excreted within known 24 h periods, derived from urinalysis monitoring, and the uncertainty associated with these values are required. These values will depend on the urinalysis method, whether a chelating agent (e.g. DTPA) was used to enhance excretion, normalisation assumptions (i.e. for non-24 h samples), etc. Strictly speaking, the measurement data needed for the final analysis consists of values of idealised theoretical 24 h excretion rates, and these need to be inferred from the actual measurement data.
- Step 2: Some pattern of exposure must be assumed based on the workers history and/or default assumptions.
- Step 3. Mathematical models which describe the entry of plutonium into the body (primarily through inhalation) and the biokinetic behaviour following entry into the body must be used. These, in conjunction with the exposure pattern from Step 2, will provide estimates of the number of disintegrations in different source regions of the body over time.
- Step 4: Dosimetry models must be used to convert the calculated disintegrations to organs doses received in each calendar year.

The report is therefore divided into sections which deal with these four steps separately:

- measurement assumptions,
- the exposure scenario,
- biokinetic modelling,
- dosimetric assumptions.

For each of these sections, the methodology, including a specification of model parameters will be given. However, the justification for the adoption of the parameter values will be given in separate papers where necessary, and appropriately referenced here.

MEASUREMENT ASSUMPTIONS

Introduction

In the final analysis, measurements of the plutonium activity in samples of a worker's urine are used to determine organ doses (together with their uncertainties). For some workers, autopsy measurements (activity in organs) are also used, but the principles outlined for urine measurements can be used. These posterior probability distributions of organ dose will depend heavily on the uncertainty attached to measurements of plutonium in individual urine samples. There are two distinct types of measurement:

- Real measurements: where a measurement is sufficiently large to enable the measurement process to make an estimate of it.
- LOD (Limit of Detection) measurements: where the activity is too small for the measurement process to reliably detect it.

It is assumed that the actual excreted amounts of plutonium, following an intake, are lognormally distributed. The median of this distribution will be referred to here as the underlying or true 24 h excretion rate, A true 24h. This section is concerned with quantifying the geometric standard deviation (or scattering factor, SF) of this lognormal distribution. A real (i.e. positive measurement) will thus be characterised by two values (the measurement and the SF).

LOD measurements are also characterised by two values. The first is the decision threshold (DT) which represents an upper bound for the measurement and the second is the SF.

In deriving the total uncertainty, many sources of uncertainty need to be considered. These can be divided broadly into those involving counting statistics on the sample itself (Type A uncertainties), and those involving a more subjective approach (Type B uncertainties). See Table 2 for examples of Type A and Type B uncertainties.

A summary of the different types of urine measurements is shown in Table 3. For Mayak Workers, measurement Types B, C and D occur.

Aim

Each real measurement of activity in urine is quantified by a median (M) and geometric standard deviation, or SF. Each LOD measurement is characterised by a single value DT and SF. The aim of this section is to show how to derive M, DT and SF from the actual measurements and the measurement processes. For further elaboration of this methodology, and to see how the equations have been applied to the Mayak data, see Vostrotin *et al.*[10].

Table 2. Examples of Types A and B uncertainties.

Type A uncertainties	Type B uncertainties
Counting statistics on the sample	Type of urine measurement made
Background counts	Failure to give a proper sample
Uncertainty in aliquot measurement	Unknown factors
Detector efficiency	Biological variation

Table 3. Different types of urine measurements.

Measurement type	Description
A True 24 h sample	This refers to samples that are carried out under rigorous scientifically controlled conditions. This level of rigour is not expected for normal routine samples supplied by workers.
B Assumed 24 h sample	These are samples that are received by a worker and are used directly without any normalisation.
C Volume normalised	These are samples that are regarded as too small (V) to have been reasonably regarded as 24 h sample, and so the measurement is scaled up in ratio V to V_{def} where V_{def} is the average amount expected to have been excreted in 24 h.
D Creatinine normalisation	These are samples that are normalised by scaling the measurement up in the ratio of C to C_{def} where C is the measured creatinine in the sample and C_{def} is the average amount of creatinine that one would expect to be excreted in a 24 h sample.
E Spot sample	This is a sample that is given from one single void and therefore has to be normalised in some way before it can be used.

'Real' Measurement data

For real measurements, the distribution (probability density) of a measurement result is a lognormal distribution characterised by two parameters: the median M and scattering factor SF. The calculation of SF requires a consideration of both Type A and Type B uncertainties.

Type A uncertainty

The sources of uncertainty contributing to the overall Type 'A' uncertainty are assumed to be normally distributed. If A_d is the activity in the whole sample, then its uncertainty is expressed as a relative standard uncertainty, RSU(A_d), and calculated according to whether the measurement was made by alpha radiometry or spectroscopy.

Alpha radiometry For Alpha radiometry, RSU(A_d) is given by:

$$\mathrm{RSU}(A_d) = \sqrt{\frac{\left(A_a\frac{V_p}{V_a}\right)^2\left(\frac{\frac{N}{t^2}+\frac{N_b}{t_b^2}}{\left(\frac{N}{t}-\frac{N_b}{t_b}\right)^2}+\mathrm{RSU}^2(\epsilon)+\mathrm{RSU}^2(V_p)+\mathrm{RSU}^2(V_a)\right)+A_{bl}^2\mathrm{RSU}^2(A_{bl})}{\left(A_a\frac{V_p}{V_a}-A_{bl}\right)^2}} + \mathrm{RSU}^2(R)+\mathrm{RSU}^2(V_d)+\mathrm{RSU}^2(V_{an}) \quad (1)$$

where:

$$\mathrm{RSU}^2(V_p) = \mathrm{RSU}^2(V_a) = \mathrm{RSU}^2(V_d) = \mathrm{RSU}^2(V_{an}) = 0.05^2.$$

The symbols are defined in Table 4.

Alpha spectrometry For alpha spectrometry, the relative standard uncertainty of Pu isotope activity (n) in a daily urine sample is calculated using:

$$\mathrm{RSU}^2(A_d^n) = \frac{(A_d^n)^2\mathrm{RSD}^2(A_d^n)+(A_{bl}^n)^2\mathrm{RSD}^2(A_{bl}^n)}{(A_d^n-A_{bl}^n)^2} + \begin{cases} 0, & \text{at analysis of complete urine sample} \\ \mathrm{RSU}^2(V_d)+\mathrm{RSU}^2(V_{an}), & \text{at analysis of fraction of collected urine sample, volume } V_{an} \end{cases}$$

$$\mathrm{RSU}^2(A_a^n) = \mathrm{RSU}_{1,n}^2 + \mathrm{RSU}_{2,n}^2 + \mathrm{RSU}^2(DPM_{\exp}) + \mathrm{RSU}^2(BR_{tr}) + \mathrm{RSU}^2(BR_n),$$

$$\mathrm{RSU}_{1,n}^2 = \frac{T_b^2\sigma^2(Cnt_g^n) + T_s^2\sigma^2(Cnt_b^n) + K^2\sigma^2(PC_n)\left(T_bCnt_{gtr}-T_sCnt_{btr}\right)^2}{\left(\begin{matrix}T_bCnt_g^n - T_sCnt_b^n - \\ PC_nK\left(T_bCnt_{gtr}-T_sCnt_{btr}\right)\end{matrix}\right)^2},$$

$$\mathrm{RSU}_{2,n}^2 = \frac{\left(T_bCnt_g^n - T_sCnt_b^n\right)^2\left[T_b^2\sigma^2\left(Cnt_{gtr}\right)+T_s^2\sigma^2\left(Cnt_{btr}\right)\right]}{\left(T_bCnt_{gtr}-T_sCnt_{btr}\right)^2\left(\begin{matrix}T_bCnt_g^n - T_sCnt_b^n - \\ PC_nK\left(T_bCnt_{gtr}-T_sCnt_{btr}\right)\end{matrix}\right)^2},$$

$$\mathrm{RSU}^2\left(DPM_{\exp}\right) = \sigma^2\left(DPM_{\exp}\right)\left(DPM_{\exp}\right)^{-2},$$

$$\sigma^2\left(Cnt_g^n\right) = Cnt_g^n,\quad \sigma^2\left(Cnt_b^n\right) = Cnt_b^n,\quad \sigma^2\left(Cnt_{gtr}\right) = Cnt_{gtr},\quad \sigma^2\left(Cnt_{btr}\right) = Cnt_{btr}.$$

Table 4. Notation used for α-Radiometry method.

Symbol	Name	Unit
N	Number of counts on alpha-radiometer detector while measuring target with plutonium precipitated from an aliquot (V_a), which was taken from the initial volume of dissolution of urine sample (V_p) taken for analysis (V_{an})	(counts)
t	Duration of Pu activity measurement using target	s
N_b	Number of background counts of α-Radiometer while measuring the pure target	(counts)
t_b	Duration of radiometer background measurement	s
ε	Registration efficiency of counts made by detector	—
A_a	Pu activity measured in an aliquot of the initial volume of sample dissolution	Bq
V_p	Initial volume of dissolution of urine sample taken for analysis	mL
V_a	Aliquot volume of initial dissolution taken for Pu measurement	mL
R	Chemical recovery	—
A_{bl}	Activity of blank urine sample of V_{an} value, which was taken from an Ozersk inhabitant who has never worked at the Mayak PA	Bq
V_d	Volume of collected urine portion submitted for radiochemical analysis	mL
V_{an}	Volume of urine taken from collected urine for Pu radiochemical analysis	mL
A_d	Pu activity in collected urine	Bq

Calculation of the relative standard uncertainty of the sum of Pu isotopes activity in the collected urine sample is propagated as shown below:

$$\mathrm{RSU}(A_d) = \sqrt{\frac{\left(A_d^{238}\right)^2 \mathrm{RSU}^2\left(A_d^{238}\right) + \left(A_d^{239}\right)^2 \mathrm{RSU}^2\left(A_d^{239}\right)}{\left(A_d^{238} + A_d^{239}\right)^2}}, \tag{2}$$

where the symbols are defined in Table 5.

Approximating Type A uncertainties by a lognormal distribution

The next step is to approximate the normal distribution which represents Type A uncertainties (mean A_d and relative standard uncertainty, RSU(A_d)), to a lognormal distribution (median M and scattering factor for Type A as SF_A) using Eqs. (3) and (4),

$$\mathrm{M} = A_d \tag{3}$$

$$SF_A = \exp\sqrt{\ln(\mathrm{RSU}^2(A_d) + 1)}. \tag{4}$$

Type B uncertainties

The sources of uncertainty contributing to the overall Type 'B' uncertainty are judgement values and associated with the type of measurement being performed. These are assumed to be lognormally distributed. The associated SFs for each type of measurement are shown in Table 6.

In some cases, it is assumed that the volume of urine in a sample is too small to be considered to be a true 24 h sample, and volume normalisation is applied. In other cases, where measurements of creatinine in the sample are made, creatinine normalisation is applied. These normalisations are both gender dependent. This subsection defines how these normalisations are made.

Volume normalisation If the volume of the urine sample V_d is less than some critical level $V_{\min}$ (=0.5 litres), then A_d (and M) is scaled up by a factor K_{vol} where

$$K_{\mathrm{vol}} = \left\{ \begin{array}{l} \frac{V_d^{\mathrm{ref}}}{V_d},\ if\ V_d < V_{\min} \\ 1,\ if\ V_d \geq V_{\min} \end{array} \right\},\quad by\ volume. \tag{5}$$

The reference volumes are sex dependent and the values used are shown in Table 7.

SF_A is assumed to be invariant to volumetric scaling.

Creatinine normalisation If the level of creatinine, C_d, in a urine sample is measured, then A_d (and M) is scaled by a factor C_{ref}/C_d where the values of C_{ref} are sex dependent and shown in Table 8.

SF_A is assumed to be invariant to creatinine scaling.

Summary of Type B uncertainty The assumed values for $\mathrm{SF_B}$ are given in Table 6. For justification for these values refer to Vostrotin *et al.*[10].

Modification for DTPA

DTPA is a chelating agent commonly used to enhance clearance of plutonium from the body—knowledge of such use is important as it enhances the rate of urinary excretion.

At Mayak, chelation therapy has only been used reactively in a relatively small number of acute

Table 5. Notation used for α-Spectrometry method.

Symbol	Name	Unit
A_d	Activity of sum of Pu isotopes in collected urine	Bq
V_d	Volume of collected urine sample (assumed daily urine sample)	mL
V_{an}	Volume of urine used for radiochemical analysis	mL
A_d^n	Activity of Pu isotope in daily urine	Bq
A_a^n	Activity of precipitated Pu isotopes from urine on the target	Bq
A_{bl}^n	Activity of Pu isotopes in blank urine sample after the subtraction of background for the measuring device	Bq
BR_n	Branching ratio (disintegration) for the isotope	(fraction)
BR_{tr}	Branching ratio (disintegration) for the tracer nuclide	(fraction)
Cnt_b^n	Spectrometer count rate in the Region of Interest (ROI) for the isotope at the time of background measurement T_b	cps
Cnt_g^n	Total count rate in the ROI for the isotope at the time of measurement T_s	cps
Cnt_{btr}	Spectrometer background count rate in the ROI for the tracer at the time of background measurement T_b	cps
Cnt_{gtr}	Total count in the ROI for the tracer at the time of measurement T_s	cps
$DPM_{\exp}$	Tracer's activity as of date of certification	Bq
K	Correction for tracer contamination decay between certification date and start of measurement T_{elapse}	—
PC_n	The tracer contamination with a corresponding isotope as of certification date	(fraction)
T_b	Time of background measurement	day
T_n	Isotope half-life	day
T_s	Time of measurement (real time) of a sample	day
T_{elapse}	Time elapsed between certification date and start of measurement	day
T_{prepare}	Time elapsed between sample provision and start of measurement	day
$\sigma()$	Standard deviation of term in parentheses	Same as parent value

Table 6. SFs for each type of measurement.

Type of measurement	Scattering factor SF_B
Assumed 24 h sample	1.7
Volume normalised	1.8
Creatinine normalised	1.6

Table 7. Reference volume excretion rates.

Sex	Reference volume excretion rate, V_{ref}^d L/d[11]
Male	1.6
Female	1.2

Table 8. Reference creatinine excretion rates.

Sex	Reference creatinine excretion rates g/d[11]
Male	1.7
Female	1.0

exposure cases. However, DTPA was also used proactively during the period 1961–74 to enhance urinary excretion to increase the possibility of finding detectable amounts of plutonium in urine for routine measurements. It is assumed that if DTPA was administered immediately prior to the sample being given, then the urinary excretion rate is enhanced by a factor X, where X is lognormally distributed with a median value of 62.3, and geometric standard deviation of 1.85[12]. Thus, in order to obtain estimates of what would have been excreted in a 24 h sample, had DTPA not been administered, the following correction factors are made.

The new median (M′) is given by:

$$M' = M/62.3, \tag{6}$$

and the SF is increased according to Eq. (7):

$$SF_B \rightarrow \exp\left(\sqrt{ln^2(SF_B) + ln^2(1.85)}\right). \tag{7}$$

Combining Type A and Type B uncertainties

The overall SF is obtained by combining Type A and Type B uncertainties as shown in Eq. (8):

$$SF = \exp\left(\sqrt{ln^2(SF_A) + ln^2(SF_B)}\right). \tag{8}$$

In the Mayak cohort, the overall SF is calculated separately from the measurement data set for each of the samples provided by each worker.

'LOD' Measurement data

LOD measurements are characterised by a single value (DT) which represents the upper bound of the underlying 24 h urinary excretion rate. The underlying true value (although unmeasurable) is assumed to also be uncertain. This uncertainty is also assumed to be represented by a lognormal distribution.

Calculation of the DT

The calculation of the DT depends on the measurement process.

Alpha radiometry For alpha radiometry, the DT is calculated[13, 14] from:

$$DT = 2.33\sigma(A_{bl})\frac{V_d}{V_{an}}, \tag{9}$$

where

A_{bl} = the average activity of Pu in an Ozersk resident (nonworker).
V_d = the collected volume
V_{an} = the volume of urine used for the radiochemical analysis
$\sigma(A_{bl})$ = the standard deviation of A_{bl}

Alpha spectrometry For alpha spectrometry, the DT is calculated from:

$$DT = 2.33 \times \sqrt{\sigma(A_{bl-238Pu})^2 + \sigma(A_{bl-239Pu})^2} \times \frac{V_d}{V_{an}}, \tag{10}$$

where the symbols are given in Table 5.

Calculation of the LOD SF

The SF associated with an LOD measurement is assumed to be represented by SF_B and the values for each type of measurement are shown in Table 6.

How measurement data is used

For any given intake, I, the biokinetic models, together with assumptions about the intake regime, are used to calculate the hypothetical urinary excretion rate (per 24 h), at times defined by the measurement data. The probability density (p) of observing an observed measurement (m) for any given intake (I), $p(m/I)$ is calculated as a measure of how far the measurement lies from the hypothetical prediction. This is often referred to as the likelihood of the intake given the measurement, and its calculation will depend on whether the measurement is real or LOD. If the measurements are independent, then the joint likelihood (of all the measurement data) will be the product of the individual likelihoods for each measurement. The likelihoods are then multiplied by an assumed prior distribution, $p(i).dI$, and Bayes theorem is used to calculate the posterior probability of intake. Organ doses are related to the intake via biokinetic and dosimetric hyper-models (described later) and by the chosen set of parameter values.

Real data

The probability of observing a real data measurement is calculated by assuming that the hypothetical measurement values are lognormally distributed around a 'true' value ($A_{24h}^{true} = I \times f[\boldsymbol{l}, t]$) which lies on the median of the lognormal distribution. The required probability is thus the height of the lognormal distribution at the measurement value,

$$P(A_{24h}|I, \boldsymbol{l}) = \frac{1}{A_{24h}\sqrt{2\pi}\ ln(SF)} \times \exp\left(-\frac{(ln(A_{24h}) - ln(I \times f(\boldsymbol{l}, t)))^2}{2ln^2(SF)}\right), \tag{11}$$

where

$I \times f(\boldsymbol{l}, t)$ = is the underlying true 24 urinary excretion rate
A_{24h} = the measurement result
I = the intake (Bq)
l = vector of parameter values used in a single iteration
$f_{(l,t)}$ = predicted 24 h urinary excretion value for the vector of parameters l at time t for unit intake
SF = the scattering factor (geometric standard deviation).

LOD data

The probability of observing an LOD measurement is also calculated by assuming that the hypothetical measurement values are lognormally distributed around a 'true' value which lies on the median of the lognormal distribution. However, in this case, the probability of observing a value <DT is the integrated area under the normal curve between DT and zero,

$$P(A_{24h}|I, \boldsymbol{l}) = \int_0^{DT} dA_{24h} \frac{1}{A_{24h}\sqrt{2\pi}\ ln(SF')} \times \exp\left(-\frac{(ln(A_{24h}) - ln(I \times f(\boldsymbol{l}, t)))^2}{2ln^2(SF')}\right), \tag{12}$$

where SF′ is the scattering factor. In practice, since it was not possible to assess Type A uncertainty for LOD data, SF′ was taken to be numerically equal to SF_B.

ASSUMED EXPOSURE SCENARIO

Introduction

An intake regime is an assumption about the time course of the rate of intake into the body (pattern), but not the actual value of the intake. An acute intake is when all of the activity enters the body at a single time and is usually associated with abnormal exposure events or accidents. A chronic intake is when the rate of intake between two times is constant (i.e. over multiple days) and mostly reflects routine exposures associated with low level contamination. A complex intake regime is when the intake rate as a function of time is a more complicated pattern; they are used to take advantage of knowledge of routine exposures in more complex exposure environments. The intake is the total amount of activity (Bq) entering the body integrated over the entire intake regime. An individual's overall exposure pattern may include one regime or multiple regimes of each of these three types.

Aim

The aim of this section is to define the intake regimes for the Mayak PA workers to be used in the MWDS-2013 analysis, and describe how uncertainty in the intake regime is assessed.

Specification of the intake regime

It has been decided that a 3-step function will be used to model the complex intake regime, based on the relative scaling of average air concentrations at Mayak facilities (1950 → 1980) with heights H1, H2 and H3 defined as:

$$\begin{aligned} \text{H1}(\leq 1957) &= 100 \\ \text{H2}(1958\text{–}1970) &= 10 \\ \text{H3}(>1970) &= 0.2 \end{aligned}$$

The uncertainties in H1, H2 and H3 are shown in Table 9.

A full justification for the choice of this three step function, and a description of how the parameter values given in Table 9 were derived is given in Sokolova *et al.*[15] in this issue. That paper also demonstrates that organ doses are relatively insensitive to the shape of the intake regime and this in turn justifies the use of requiring only three steps.

Dealing with Multiple intakes

Where direct evidence points to additional acute intakes at specific times, the worker has been excluded from the epidemiological analysis for historical reasons. In principle, there is no reason why such workers should be excluded in the cohort, and it is proposed to investigate this further in a future study.

Dealing with work history

In cases where a worker has worked for separate periods of time, the work history is convoluted with the three step function to form a unique complex intake regime for that individual. Further details are given in Sokolova *et al.*[15] in this issue; details of how a complex intake regime is implemented mathematically for dose reconstruction are provided by Puncher *et al.*[2].

Dealing with mixtures

Three plutonium compounds are considered:

- Oxides
- Nitrates
- Mixtures

Oxides and nitrates have their own specific dissolution parameters which are discussed later in this paper. Compounds described as mixtures are treated as a physical mixture by activity: f oxides and $(1-f)$ nitrates.

Since there is no information on f, a uniform prior distribution is assumed, based on the fact that it does not favour any specific value (Table 10).

Prior Distribution on the Intake

The prior distribution on intake itself (Bq) is represented by a lognormal distribution with a median

Table 9. Parameters of the step function used for the intake regime for Mayak workers.

Parameter	Distribution	Parameters of distribution			Default values	Shared or unshared
		a	*b*	*c*		
H1	Log-uniform	10	1000	—	100	Shared
H2	Log-uniform	1	100	—	10	Shared
H3	Log-uniform	0.1	0.4	—	0.2	Shared

Table 10. Definition of parameter *f* which determines the fraction of oxide in the mixture.

Parameter	Distribution	Parameters of distribution			Default value	Shared or unshared
		a	*b*	*c*		
f	Uniform	0	1	—	0.5	Shared

Table 11. Parameters of the lognormal prior distribution.

Parameter	Distribution	Parameters of distribution			Default value	Shared or unshared
		a	*b*	*c*		
Intake	Lognormal	M	6	—	M	Unshared

value (M) that increases with the length of employment. The parameters are shown in Table 11.

The value of the geometric standard deviation is chosen so that the prior distribution is uninformative on the actual intake, except for situations in which the measurement data is very sparse. The value of M is based on air sample measurements. The lognormal distribution with variable median M and GSD of six is based on one derived by Puncher *et al.*[16] from an analysis of historical personal air sampler data relating to plutonium and uranium concentrations in former workplaces of the UK Atomic Energy Authority. That paper also includes a sensitivity analysis on M to lung dose; it was found a 10-fold change in M gave a 2-fold change in lung dose, indicating that dose estimates are not overly sensitive to the choice of the value of M. This is also likely to be the case for Mayak workers who have broadly similar quality urine data to the UKAEA workers considered by Puncher *et al.*[16] in their analysis.

For Mayak PA workers, three separate time periods are identified by Sokolova *et al.*[15] where average air concentrations are expected to be different:

$i = 1$ corresponds to the time period before end of 1957
$i = 2$ corresponds to the time period 1958 → 1970
$i = 3$ corresponds to the time period after 1970

It has been shown[15] that the average relative concentrations in these periods can be represented by:

$$\begin{aligned} \text{H1}(\leq 1957) &= 100 \\ \text{H2}(1958\text{–}1970) &= 10 \\ \text{H3}(>1970) &= 0.2 \end{aligned}$$

M (Bq) is given by:

$$M = 80 \sum_{i=1}^{3} [Y_i H_i], \tag{13}$$

where Y_i is the number of years of chronic exposure in period *i*.

BIOKINETIC MODELS

Introduction

In order to calculate organ doses, it is necessary to define the deposition and subsequent biokinetic behaviour of the plutonium after entering the body. This is done using biokinetic models for the respiratory tract, the gastrointestinal (GI) tract and systemic tissues. The structure of these models are largely based on those being developed for the forthcoming ICRP recommendations[17], but go beyond these models, as they explicitly deal with uncertainty. As mentioned in the introduction, this is done by assigning a probability distribution (prior) to the important rate constants, rather than a single value. Random values are chosen from these prior distributions for each realisation of doses, and the full collection of realisations model the uncertainty. Parameters which are shared between workers will have the same within a realisation.

Aim

The aim of this section is to define probability distributions (and representative values) for each of the important parameters used in the calculations and indicate whether they are shared or unshared.

Respiratory tract model

Deposition

A deposition model is required to determine the fractional deposition in each of the respiratory tract

compartments shown in Figure 1. To calculate regional deposition (Deposition fraction in ET, BB, bb and AI), a modified version of the ICRP Publication 66[18] deposition model is used[19]. This modification has a different treatment of deposition and clearance from the extrathoracic region based on experimental data from Public Health England, and has been incorporated in the forthcoming recommendations of the ICRP (Occupational Intakes of Radionuclides, Part 1)[17]. Although this is likely to have a negligible effect on calculated doses, it was decided to use this model for consistency.

The parameter values, together with their uncertainties, and whether they are assumed to be shared or unshared between workers are shown in Table 12. A full justification for all of the parameter values and uncertainties is given by Puncher *et al.*[20].

The revised deposition model gives the total deposition fraction within each lung region x, TOTDEP (x). Deposition within the extrathoracic region is calculated as follows:

$$\mathrm{DEP(ET1)} = \mathrm{TOTDEP(ET1)}$$
$$\mathrm{DEP(ET2)} = 0.998 * \mathrm{TOTDEP(ET2)}$$
$$\mathrm{DEP(ETseq)} = 0.002 * \mathrm{TOTDEP(ET2)}$$

To be consistent with the revised ICRP Publication 66 model[19], the partitioning between ET1 and ET2

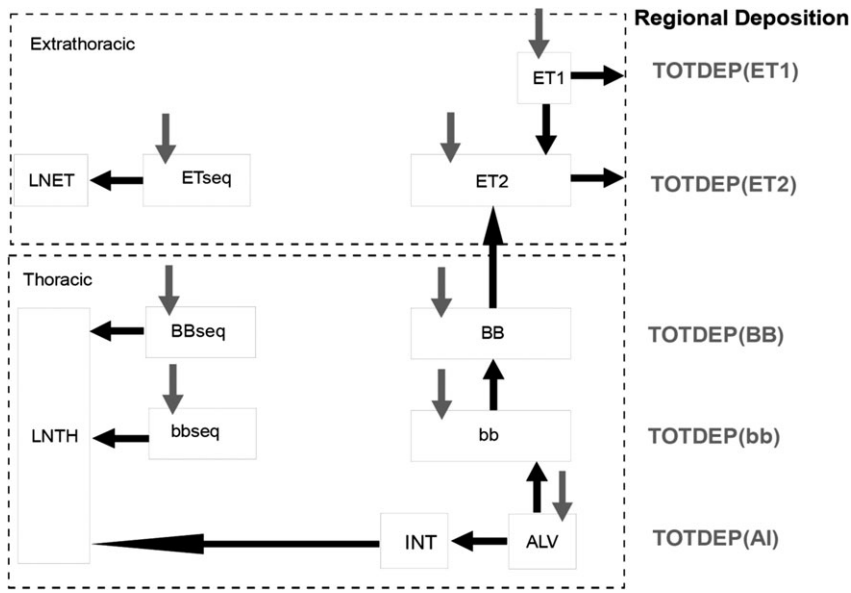

Figure 1. Respiratory tract regions for which deposition fractions (vertical arrows) are required.

Table 12. Deposition parameter distributions.

Parameter	Distribution	Parameters of distribution			Default values	Shared or unshared
		a	*b*	*c*		
AMAD	Lognormal	4.4	1.8	—	4.4	Shared
GSD	Lognormal	2.2	1.5	—	2.2	Shared
B (ventilation rate)	Lognormal	1.2	1.7	—	1.2	Unshared
ρ	Fixed	3	—	—	3	Shared
X	Fixed	1.5	—	—	1.5	Shared
f_R (respiratory frequency)	$f_R = 7B + 8$	$f_R = 7B + 8$	—	—	16.4	Unshared
f_N (fraction breathed through nose)	Triangular	0.4	1	1	0.82	Unshared
ET_1, ET_2 aerodynamic filter efficiency	Lognormal	1	1.82	—	1	Unshared
ET_1, ET_2 thermodynamic filter efficiency	Lognormal	1	1.18	—	1	Unshared

is assumed to be 0.65 to 0.35, and the sequestered fraction is now assumed to be 0.2%; i.e. TOTDEP (ET1) = 0.65 ∗ TOTDEP(ET) and TOTDEP(ET2) = 0.35 ∗ TOTDEP(ET).

Deposition in each thoracic compartment is then calculated from:

DEP(BB) = 0.998 ∗ TOTDEP(BB)
DEP(BBseq) = 0.002 ∗ TOTDEP(BB)
DEP(bb) = 0.998 ∗ TOTDEP(bb)
DEP(bbseq) = 0.002 ∗ TOTDEP(bb)
DEP(ALV) = TOTDEP(AI)
DEP(INT) = 0

Particle transport

The updated particle transport clearance model for the respiratory tract adopted by ICRP[17] and used in MWDS-2013 is shown in Figure 2. There are three main changes from the model currently recommended for radiological protection[18]. The first is a change in the way that particle transport occurs in the extrathoracic region. Justification for this approach is provided by Smith *et al.*[19]. It has been also been shown that slow clearance of particles in the bronchiolar region (bb) applies to only a small fraction material deposited there[21, 22] and so this, combined with a desire to simplify the model has resulted in removal of the slow cleared fraction completely in the upper airways. A possible slow clearance of some of the deposited activity is compensated by the decrease in clearance rates in this region. Finally, in the deep lung (alveolar region) a more realistic and generally slower rate of clearance has been adopted by ICRP, which is based mainly on the work of Gregoratto *et al.*[23].

There is clear evidence that the variability in clearance in all three regions of the respiratory tract is around an order of magnitude at the 95% confidence level[18]. Furthermore, this uncertainty appears to be lognormal. The representative values chosen for the model's rates were considered to be representative of the median values of the measurement data. Therefore, for MWDS-2013, to represent uncertainty for any individual worker, each rate constant in the extrathoracic and upper airways is multiplied by a random variable K_{PT} sampled from a lognormal distribution with a median of 1 and geometric standard deviation of 1.73. Uncertainty in clearance from the alveolar region is taken directly from that quantified by Gregoratto *et al.*[23]. The parameter values and their uncertainties are given in Table 13.

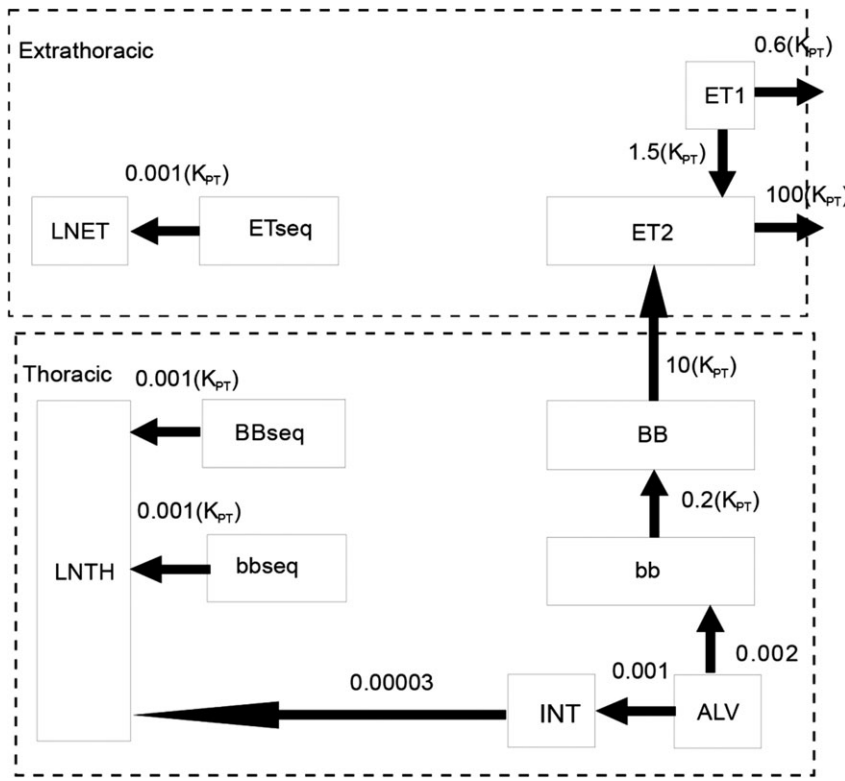

Figure 2. Representation of particle transport within the respiratory tract (units are d^{-1}).

Table 13. Treatment of uncertainty in particle transport parameters in the deep lung.

Parameter	Distribution	Parameters of distribution			Default value
		a	*b*	*c*	
ET, BB and bb region					
K_{PT}	Lognormal	1	1.73	—	1
Al region					
ALV to bb	Lognormal	0.0013	3.2	—	0.002
ALV to INT	Lognormal	0.001	4.5	—	0.001
INT to LNTH	Lognormal	0.00003	3	—	0.00003

Uncertainty in particle transport rates is modelled using a random variable K_{PT} defined in Table 13. Uncertainty in alveolar clearance is treated explicitly.

Absorption

Absorption from all regions (depicted in Figure 3) of the respiratory tract (except ET1) is assumed to follow the model shown in Figure 3[17].

All absorption parameters are assumed to depend on the physico-chemical properties of the inhaled material and are thus considered to be 100% shared between workers. There is no information contained within the Mayak data that gives information on the rapid phase of dissolution (fraction f_r and rate s_r) and so values were determined from a literature search and have been published previously[20]. Absorption parameter values for plutonium compounds have also been collated by Davesne *et al.*[24], who considered a wider range of data and obtained values that supported those derived by Puncher *et al.*[20]. In the absence of additional information for Mayak workers, the values of f_r and s_r obtained by Puncher were used for MWDS-2013. These values are shown in Table 14.

The values of the slow rate constant s_s for nitrates and oxides were determined separately. However, since binding occurs after dissolution, and the ions would have no knowledge of their previous chemical state, it can be assumed that the value for f_b is the same for nitrates and oxides. Extracting parameter values for the bound fraction (f_b and s_b) and for the slow dissolution rates proved very difficult despite the complex analytical tools available, and some judgement was ultimately required. To aid clarity, binding and dissolution are dealt with separately in the following subsections.

Binding Because the likely fraction of material bound to the respiratory tract is small, and measurement data is extremely limited, the value of s_b was constrained to be zero. Although f_b is small, it can have a significant effect on lung dose. It has been shown that if the bound fraction is 8%[25] then the effect on lung dose is profound, especially for nitrates. It has been shown that such a bound fraction would increase the dose to the bronchial basal cells by over two orders of magnitude[26]. It is thus important to quantify this fraction as accurately as possible.

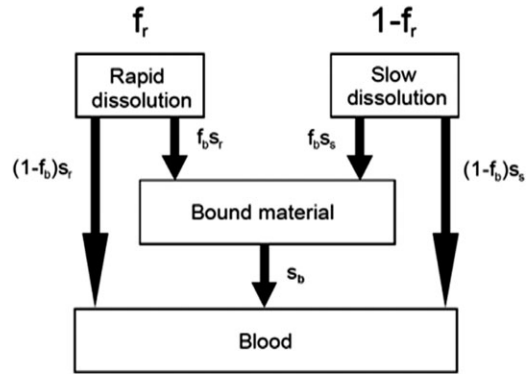

Figure 3. Absorption from the respiratory tract. A fraction *fr* of the initially deposited activity dissolves at a rapid rate, s_s while the complementary fraction dissolves at a slower rate s_s. A fraction f_b becomes bound to lung tissue where it is absorbed to blood at a much slower rate s_b.

The measurement data used to quantify f_b was taken from:

- A re-analysis of historic beagle dog data
- A re-analysis of a United States Transuranium and Uranium Registries (USTUR) case 0269
- Mayak worker autopsy data.

It was decided that the best available data for quantifying the bound fraction was contained within those Mayak Workers who had a known history of exposure to nitrates and who had also been autopsied. A Bayesian analysis was used to determine posterior distributions of f_b. However, a major problem was that the data could be explained by both the presence and absence of a bound state. The strategy was thus to use additional data from beagle dogs and case 0269 to demonstrate the existence of a bound state, and then use the Mayak autopsy data to quantify f_b having assigned it an appropriate relatively uninformative prior.

Table 14. Summary of bound fraction (f_b) values.

Data source	Bound fraction (f_b) %	Comment
Beagle dogs	0.2	ICRP-66 model structure
	0.8	MWDS-2013 model structure
USTUR	0.4	DTPA corrected
Mayak nitrate workers	0.14	Range 0.01 0.3

A full description of the re-analysis of the beagle dog data is given in this special edition[27]. The analysis was performed using two different representations of particle transport from deep lungs: one based on a dog model similar to the ICRP Publication 66 model, and one based on the MWDS-2013 model. The results yielded best estimates of 0.2% and 0.8% for f_b, respectively. For the model based on the ICRP Publication 66 structure, the model could not be explained without the presence of a bound state. For the model based on the MWDS-2013 structure, the model could be made to fit the data, but only by reducing particle transport rates to an implausible level. Taken together, the results give very strong evidence to support the presence of a bound fraction.

As part of the work undertaken by the Project 2.4 team, additional measurements of activity of plutonium in the upper airways of the lungs for USTUR case 0269 were made. A full description of the measurement procedure and results are given by Tolmachev *et al.*[28] in this issue. The results revealed a larger than expected proportion of nitrate activity remaining in the upper airways 38 years after an acute exposure to plutonium nitrate aerosol. Given that this activity would have cleared by mucociliary particle transport very quickly is strong evidence for binding (bound material is assumed to not be subject to particle transport clearance). Furthermore, this is the only case where such activity has been directly measured in the upper airways, and this is where the majority of the lung dose is delivered. A full Bayesian analysis (both including and excluding a bound fraction) of this data together with the previously published data for this case was undertaken and is described by Puncher *et al.*[29] in this issue. The analysis was performed on the actual data, and on the data corrected for DTPA administration[25]. It was concluded that the data could not be explained by the model without the inclusion of a bound fraction unless the rate of particle transport clearance from the upper airways is reduced by an unrealistic three orders of magnitude. The best estimate of the bound fraction was 0.71% for the uncorrected data. However, when the data was corrected for DTPA enhancement the best estimate of f_b reduced to 0.37%[29].

As noted above, given that both the beagle data and USTUR re-analysis indicate the existence of a bound fraction, the next step is to quantify it using the Mayak autopsy data with the assumption that a bound fraction exists (although unknown). A full description of this analysis is given by Puncher *et al.*[30] in this issue and a brief summary is reproduced here. The data was gathered from 20 Mayak PA workers who had been exposed to pure plutonium nitrate during their work history, and who had subsequently agreed to provide autopsy samples. For comparison, 20 workers exposed to pure oxide were also analysed, although it was expected that these workers would not provide as precise an estimate because of the much lower solubility of oxide compared with nitrate.

The analyses were performed using the Markov Chain Monte Carlo (MCMC) method described by Puncher and Birchall[1] and Puncher *et al.*[2]. The MCMC routines use the software IMBA Professional Plus[6] to calculate bioassay predictions. This MCMC method is an implementation of the single component Metropolis algorithm[31].

The data used was plutonium activity measured in liver, skeleton, daily urinary excretion rates, lung and lymph contents. A full description of the derivation of these activities from autopsy samples is given by Suslova *et al.* and Sokolova *et al.*[32, 33] in this issue. Since it can be assumed that the majority of systemic activity travels either to bone or liver (~90%), the liver and skeleton activities were added to provide a single measurement of systemic uptake which avoided redistribution uncertainty between these two organs.

The prior distributions representing variability in macrophage mediated particle transport clearance from the deep lung were taken to be those specified in the MWDS-2013 model (Table 13). Other particle transport parameters were assumed to be fixed ($K_{PT} = 1$) as they did not affect the analysis. The intake was allowed to vary uniformly between 1 and 106 Bq, and the parameters s_s and f_s were chosen to be uninformative (0–0.1 and 0–1, respectively). The prior for f_b was chosen to be uniform between 0 and 1. This distribution shows no preference for one parameter value over another and its use was justified on the basis that it was assumed that there are currently no reliable estimates of f_b from other studies that could form the basis of an informative prior for this parameter. The analysis was performed by constraining the bound fraction and absorption parameters

to be shared between workers while the particle transport rate and intake were allowed to vary between individuals. The resulting posterior distribution for the oxides gave an estimated value of f_b (arithmetic mean) of 4.7% but as expected the uncertainty on this fraction was large (95% range from 0.27% to 10.6%). Conversely, the nitrate data gave a more precise estimate of f_b of 0.14% with a 95% credible interval between 0.011% and 0.3%. The resulting posterior probability for f_b is shown in Figure 4. A summary of the bound fraction estimates discussed so far are given in Table 14.

Inevitably, the choice of prior has to include some measure of judgement. It should be noted that the beagle dog data was non-human; the USTUR data was for only one individual, whereas the Mayak data contained information on 20 workers exposed to the nitrate of interest. In choosing the final distribution to represent uncertainty in bound fraction f_b, more weight was therefore given to this data set. The final decision, made by the Project 2.4 team after much deliberation, was to use a uniform distribution between 0 and 0.4% with a representative value of 0.2%. It is expected that this value will also be adopted in the forthcoming ICRP recommendations for all actinides.

Slow dissolution The absorption model is shown in Figure 3. As stated previously, this section is concerned with determination of the slow rate of clearance, s_s, only. A sensitivity analysis carried out internally by the Project 2.4 team has shown that lung doses are very sensitive to this parameter. It is proposed to deal with oxides and nitrates separately.

Oxides As noted in the previous section, early estimates of s_s for oxides have been derived previously based on a literature search of available data[20]. Here it was concluded that s_s could be adequately represented by a lognormal distribution with a median value of 9.5 10^{-5} d^{-1} and a geometric standard deviation of 4.2. This study was mainly based on short term animal studies and resulted in a high degree of uncertainty. For MWDS-2013, values were derived directly from the Mayak PA autopsy data. A summary of the main results is presented here and a complete description is presented by Puncher *et al.*[34] in this issue.

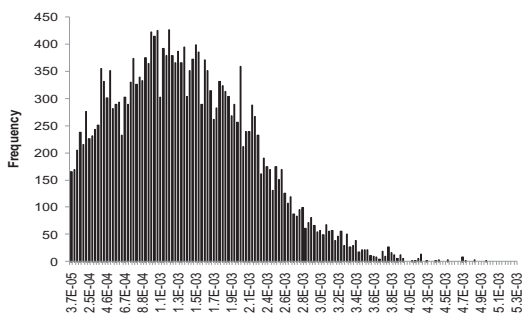

Figure 4. Posterior distribution for f_b based on the nitrate data.

The data consists of autopsy measurements of plutonium at time of death in liver, skeleton, lung and lymph nodes[32, 33] for 20 workers deemed to have been exposed to oxides only. For convenience, lung and lymph nodes are added to form a single data point, as are liver + skeleton. The WeLMoS method[1] was used to obtain estimates of s_s separately for each worker, and then Markov Chain Monte Carlo[2] was used to obtain a single best estimate of the posterior probability distribution of s_s from a simultaneous analysis of all 20 workers while treating shared and unshared parameter values separately. The pattern of exposure was obtained by convoluting the workers' history with the 3-step intake function[15], and a uniform prior on the total intake (I) was assumed: $I \sim U(0, 106)$. Additional priors on particle transport rates from the alveolar region were taken from Table 13, and an uninformative prior attached to the value of s_s itself.

Interestingly, the analysis of s_s which treated each worker separately (i.e. ignoring the fact that s_s is shared between all workers) led to a bias by a factor of 2.4 in the arithmetic mean (11.0 10^{-5} d^{-1}) compared with the MCMC analysis which gave a mean of 4.69 10^{-5} d^{-1}. This is discussed further in Puncher *et al.*[34]. In this analysis, the bound fraction was set to zero. However, it has been shown[30] that the introduction of a bound state for oxides has a negligible effect on the estimation of s_s, and so it was concluded that s_s can be best represented by a lognormal distribution with a median value of 4.7 10^{-5} d^{-1} and a geometric standard deviation of 1.07. Note the reduction in the geometric standard deviation σg compared with the literature survey ($\sigma g = 4.2$).

Nitrates The determination of s_s for nitrates proved one of the most difficult tasks, partly because of interference by other competing parameters (particle transport, sequestration), and partly because of different values arising from different studies. A previous study resulting from a literature search[20] showed that the estimates of s_s were lognormal $s_s \sim LN(12\ 10^{-4}, 2.3)$. However, this work was based mainly on animal studies. In this study, three sources of data on humans were considered:

The first source of data was the results of a two-volunteer study carried out at Public Health England (formerly the National Radiological Protection Board NRPB) where subjects both inhaled and were injected with plutonium isotopes. Although only two volunteers were used, the measurement results were extensive and scientifically controlled. This study is described elsewhere[35]. Early estimates of s_s were in

the order of 12 10^4 d^{-1}, but a more recent and thorough analysis carried out within the EU funded SOLO project has shown that s_s can be represented with a best estimate (arithmetic mean) of 22 10^{-4} d^{-1} (95% range 19–23 10^{-4} d^{-1}) (Puncher and Etherington, in prep).

The second source of data was taken from a re-analysis of the USTUR case 0269. This case is referred to earlier in the section on binding, and is covered in detail by Puncher *et al.*[29] in this issue. The original data could be explained with either binding or no binding. If binding is assumed in the Bayesian analysis, as demonstrated in a previous section then a value of 10 10^{-4} d^{-1} is obtained (it is interesting to note, that if binding is excluded, $f_b = 0$, then a much lower value of three 10^{-4} d^{-1} is obtained). Further measurements were made on this subject, which included measurements of plutonium activity in the upper airways, and when these are included in the Bayesian analysis, then a value of 24 10^{-4} d^{-1} is obtained. Correcting this data to account for DTPA elimination from organs following administration results in an even higher estimate of 48 10^{-4} d^{-1}.

In summary, values of s_s coming from an analysis of two human volunteers at PHE, and an analysis of one accidental exposure from the USTUR database results in estimates of s_s in the range 10–40 10^{-4} d^{-1}. These results are also consistent with values derived from a literature search (12 10^{-4} d^{-1}), but these were based mainly on animal experiments. For this study, it was decided that the best source of data was from an analysis of 20 Mayak workers who had been exposed to plutonium nitrate and who had subsequently been autopsied.

A full analysis of this data is presented by Puncher *et al.*[34] in this issue, and so only the results will be presented here. Basically, the methodology was exactly the same as that described in the previous subsection for the Mayak oxide exposures. The best estimates of s_s for all 20 Mayak cases were quite consistent and centred around a much slower estimate of 2.4 10^{-4} d^{-1}. For the MCMC analysis which is a simultaneous analysis that constrains s_s to be shared for all 20 workers, a similar estimate of 2.58 10^{-4} d^{-1} was obtained with a very narrow range (95% CI: 2.31–2.78 10^{-4} d^{-1}).

It was difficult to decide on a final posterior distribution for s_s to be used as the prior distribution for the final MWDS-2013 analysis because of these different estimates. The combined estimate from the 20 Mayak nitrate cases resulted in a much lower value than the other three cases considered here (2 from the PHE experiment and 1 from the USTUR registry). However, it was considered that the 20 Mayak cases, who were exposed to the material of interest in this study, provided the best quantitative data on which to provide a realistic estimate of s_s. Furthermore, these estimates were remarkably consistent between individual workers. It was therefore concluded that for MWDS-2013, that $s_s \sim$ LN (2.5 10^{-4} d^{-1}, 1.08).

This being said, it is considered that this topic should be kept under critical review. One major difference between the data from both the PHE experiment and the USTUR case and that of the 20 Mayak workers is that the former measurement data occurs at times shortly after exposure, whereas the Mayak data is based on measurements taken many years after the intake. If for example, the absorption rate changed from a relatively fast rate early on to a slower rate at later times many years after exposure, then this could lead to the observed results. Alternatively, a mechanism whereby absorption is slower from the interstitial region than other regions may also explain the apparent discrepancy. What is clear is that given the current clearance structure of the MWDS-2013 model, the data from early measurements is inconsistent with those obtained at later times. A full analysis (simultaneous fit of early and late data) was beyond the scope of this current work, but in view of the extreme sensitivity of lung dose to this parameter[26] it will be important to investigate this problem further in the future.

Summary of absorption parameters A summary of all the prior distributions derived for the absorption parameters is shown in Table 15.

GI Tract model

Organ doses calculated from urine measurements are extremely insensitive to the structure of the GI tract model. Therefore, to model activity that is ingested, or cleared to the stomach via particle transport from the lungs, the ICRP Publication 30 GI Tract Model[36] is used. For completeness, the structure is shown in Figure 5 and the parameter values are shown in Table 16.

The f_1 fraction, defined as the fraction of activity passing through the small intestine that goes to blood (via rate constant λ_B) is given in Table 17 for both oxides and nitrates.

Systemic model

Once activity reaches the blood, either from absorption from the respiratory tract or GI tract, the biokinetics is described by the model shown in Figure 6 which is based on the Leggett Systemic Model for Plutonium[37]. A critical validation of this model for calculating doses to organs based on data from both urine and autopsy data is presented in this issue[38].

The parameter values describing the biokinetic behaviour between compartments are fixed and taken directly from the Leggett model (Table 18).

In order to model uncertainty in activity reaching liver and skeleton, a parameter B, which multiplies

Table 15. Absorption parameters[a] for oxides and nitrates.

Parameter	Distribution	Parameters of distribution			Default values	Shared or unshared
		a	*b*	*c*		
			Nitrate			
f_r	Right truncated lognormal	0.17	2	1	0.2	Shared
s_r	Lognormal	1	4	—	1	Shared
s_s	Lognormal	2.5E-4	1.08	—	2.5E-4	Shared
f_1	Constant	1.0E-04	—	—	1.0E-04	Shared
			Oxide			
f_r	Right truncated lognormal	0.0026	3.1	1	0.0026	Shared
s_r	Lognormal	1	4	—	1	Shared
s_s	Lognormal	4.7E-5	1.07	—	4.7E-5	Shared
f_1	Constant	1.0E-04	—	—	1.0E-04	Shared
			Bound fraction (oxide and nitrate)			
f_b	Uniform	0	0.004	—	0.002	Shared
s_b	Constant	0	—	—	0	Shared
f	Uniform	0	1	—	0.5	Shared

[a] f_r is the fraction dissolving rapidly at a rate s_r while the complementary fraction dissolves more slowly at a rate s_s. f_1 is the fraction of activity passing through the GI tract that is absorbed to blood. f_b is the bound fraction which is absorbed to blood at a rate s_b and f is the fraction of oxide assumed in a mixture of oxides and nitrates.

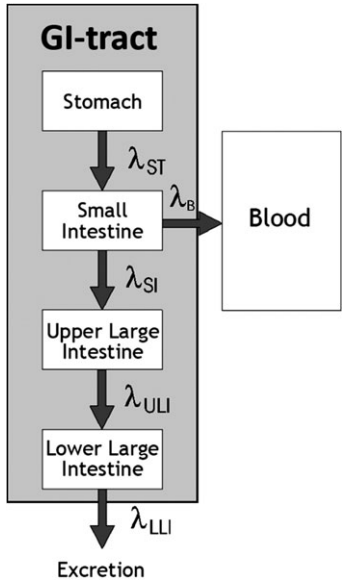

Figure 5. The GI tract model.

the rate constants from Blood to Skeleton, has been introduced[39]. In addition, in order to conserve the total amount of material transferred to Liver + Skeleton from Blood at any time (i.e. = 0.693 d^{-1}) , the rate constant from Blood to Liver is simultaneously adjusted in the model. The distribution of *B* is given in Table 18 and the rate constants used are shown in Table 19.

Combing the biokinetic models

For transparency, the combined respiratory, GI tract and systemic models are shown in Figure 7.

DOSIMETRY ASSUMPTIONS

Introduction

The dosimetric models used in the calculation of organ doses will be those currently recommended by ICRP to calculate doses for workers[40]. Although ICRP are currently revising their recommendations on Specific Absorbed Fractions (SAFs), and updating the nuclear database on energy emissions, the resulting new specific effective energies (SEEs) will have a negligible effect on organ doses from plutonium, with the possible exception of GI tract and bone dose.

Aim

The aim of this section is to summarise the dosimetric assumptions used to calculate organ doses.

Table 16. The GI tract model parameters.

Parameter	Distribution	Parameters of distribution (d^{-1})			Default values	Shared or unshared
		a	*b*	*c*		
λ_{ST}	Fixed	24	—	—	24	N/A
λ_{SI}	Fixed	6	—	—	6	N/A
λ_{ULI}	Fixed	1.8	—	—	1.8	N/A
λ_{LLI}	Fixed	1	—	—	1	N/A

Table 17. The f_1 values for absorption to blood from the GI tract.

Parameter	Distribution	Parameters of distribution (d^{-1})			Default values	Shared or Unshared
		a	*b*	*c*		
Nitrates						
f_1	Fixed	1.0×1.0^{-4}	—	—	1.0×1.0^{-4}	N/A
Oxides						
f_1	Fixed	1.0×1.0^{-5}	—	—	1.0×1.0^{-5}	N/A

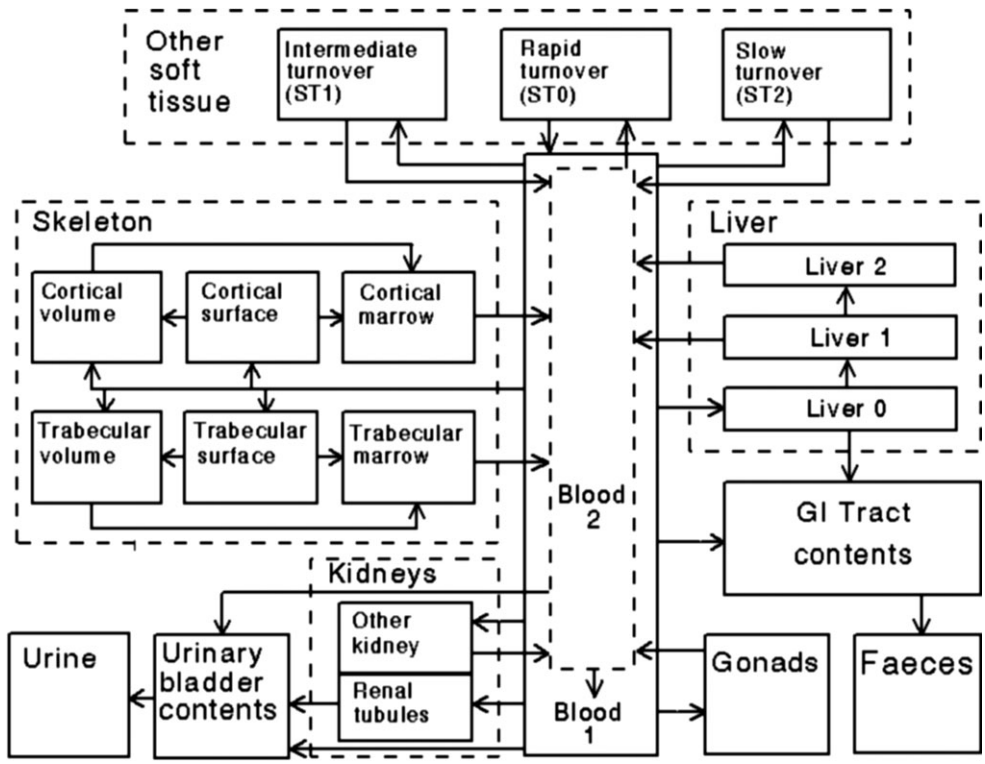

Figure 6. The systemic behaviour of plutonium after reaching blood.

Table 18. Value of *B* to deal with variation in total amounts transferred to liver and skeleton.

Parameter	Distribution	Parameters of distribution			Default value	Shared or Unshared
		a	*b*	*c*		
B	Nognormal	1	1.3	—	1	Unshared

Table 19. Rate constants used in the systemic model for plutonium.

Systemic model rate constants (d^{-1})		
From	To	Leggett
BLOOD2	UBC	3.5E+00
BLOOD2	ST0	2.895E+01
BLOOD2	BLOOD1	6.755E+01
BLOOD1	LIVER0	4.62E-01
BLOOD1	CS	8.778E-02
BLOOD1	CV	4.62E-03
BLOOD1	TS	1.247E-01
BLOOD1	TV	1.386E-02
BLOOD1	UBC	1.54E-02
BLOOD1	RT	7.7E-03
BLOOD1	OK	3.85E-04
BLOOD1	TESTES	2.695E-04
BLOOD1	OVARIES	8.4700E-05
BLOOD1	ST1	1.851E-02
BLOOD1	ST2	2.31E-02
BLOOD1	RC CONT	1.155E-02
BLOOD	BLOOD1	7.0000E+03
BLOOD	ST0	3.0000E+03
LIVER0	SI CONT	9.242E-04
LIVER0	LIVER1	4.529E-02
LIVER1	BLOOD2	1.5200E-03
LIVER1	LIVER2	3.8000E-04
LIVER2	BLOOD2	1.2660E-04
OK	BLOOD2	1.2660E-04
RT	UBC	1.733E-02
UBC	URINE	1.2000E+01
ST0	BLOOD1	9.9000E-02
ST1	BLOOD2	1.3860E-03
ST2	BLOOD2	1.2660E-04
TESTES	BLOOD2	3.8000E-04
OVARIES	BLOOD2	3.8000E-04
CS	CM	8.2100E-05
CS	CV	2.0500E-05
CM	BLOOD2	7.6000E-03
TS	TM	4.9300E-04
TS	TV	1.2300E-04
TV	TM	4.9300E-04
TM	BLOOD2	7.6000E-03
CV	CM	8.2100E-05

Treatment of beta and gammas

In order to simplify the calculations, only the alpha particle emissions are considered in the calculation of doses. This reduces the complexity and decreases the calculation time without introducing any significant error in the doses.

Alpha recoil

The energy imparted to the parent nucleus when an alpha particle is emitted is considered explicitly in the calculations of dose. This typically increases doses by about 2%.

Isotopic composition

For simplicity, and since the isotopic composition of the inhaled plutonium was unknown, it is assumed that all of the measured alpha emissions (counts) come from Pu-239. Since all Pu isotopes will behave the same kinetically, and since the half lives are all very long, and the energies of the emissions are similar, this should not introduce a significant error. Inside the lung, it is assumed that all of the isotopes (Pu-238, Pu-239, Pu-240 and Pu-241) are bound within the Pu-239 matrix and are absorbed to blood at the same rate. Pu-241 is a beta emitter which decays into an alpha emitter Am-241. For simplicity, it is assumed that the absorbed Am behaves biokinetically like Pu, but it has been shown that the possible error in dose estimates caused by this false assumption is unlikely to exceed 10%. In early years, nearly half of the cohort was involved in the production of weapons grade Pu of which the dominant component was Pu-239.

Use of organ masses

It was decided to use ICRP reference organ masses for dosimetry calculations and NOT to adjust the organ masses according to the weight of actual individuals (as is done in DOSES-2005 and MWDS-2008). However, different reference masses are used for male and female workers. A full justification for this approach is given by Birchall and Sokolova[41] in this issue.

The reference organ masses are reproduced here for completeness in Table 20.

For practical implementation, doses are calculated for the male worker, and the female organ doses are simply obtained by multiplying by the male organ doses by the ratios given in Column 5 of Table 20. Note that the biokinetic model for male

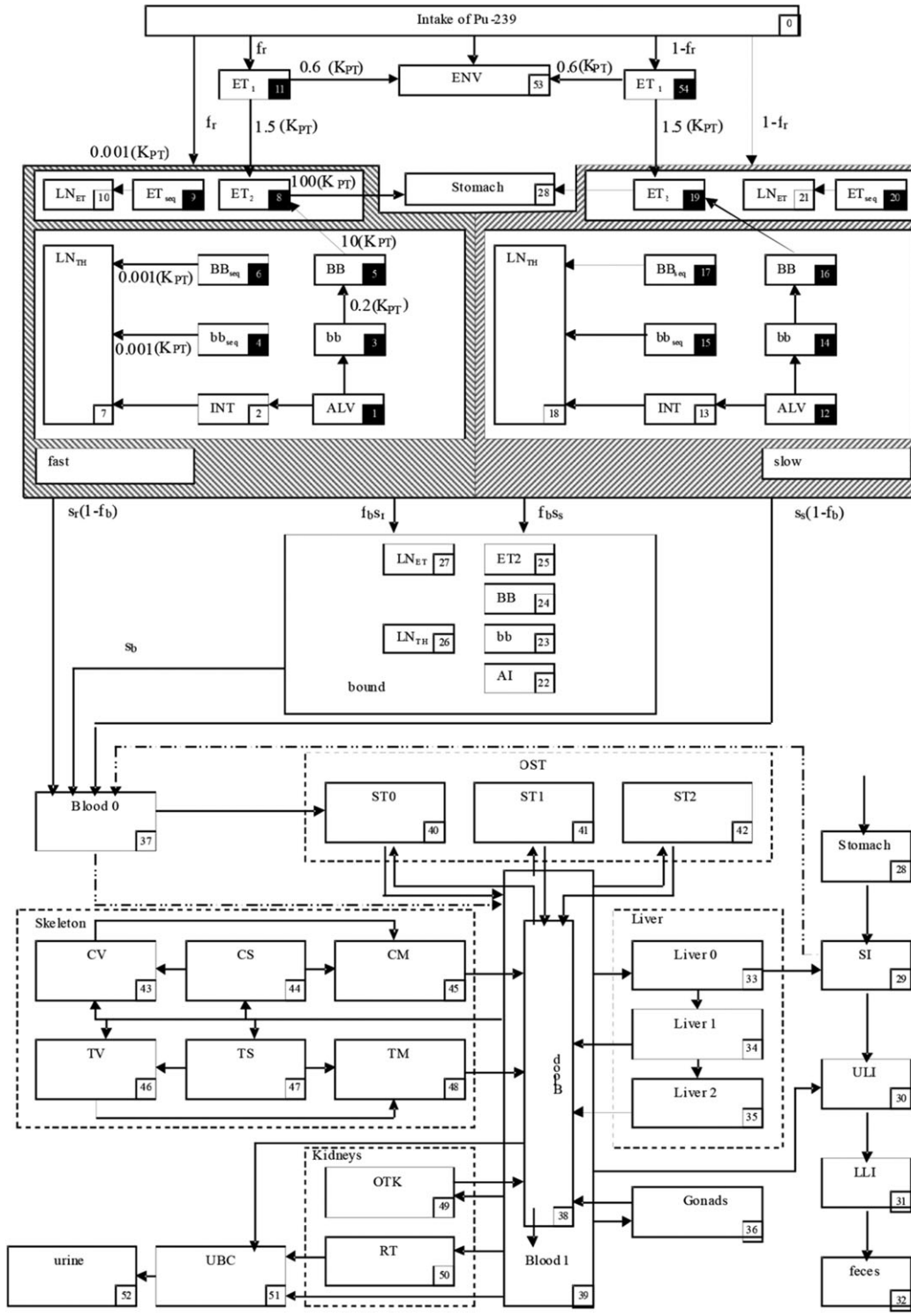

Figure 7. Combined biokinetic model for plutonium.

Table 20. Reference male and female organ masses used for the scaling of dose.

Organ or tissues	Mass of organ or tissue (M), g			Ratio M_M:M_w
	ICRP references	Reference man	Reference woman	
Alveolar-interstitial region (AI)	66	1100	904	1.2168
Bronchi basal cells (BB_{bas})	66	0.432	0.390	1.1077
Bronchi secretory cells (BB_{sec})	66	0.865	0.780	1.1090
Bronchiole secretory cells (bb)	66	1.95	1.90	1.0263
Lung lymph nodes (LN_{TH})	66	15	12.3	1.2195
Liver	23	1800	1400	1.2857
Bone surface cells	23,30	120	90	1.3333
RBM	23	1500	1300	1.1538
Gonads	23	35	11	3.1818
Kidneys	23	310	275	1.1273
Urinary bladder walls (UBWALL)	23,30	45	35.9	1.2535
Stomach walls (STWALL)	23,30	150	140	1.0714
Small intestine walls (SIWALL)	23,30	640	600	1.0667
Upper large intestine walls (ULIWALL)	23,30	210	200	1.05
Lower large intestines walls (LLIWALL)	23,30	160	160	1
Other soft tissues (ST0+ST1+ST2)	23	58 700	49 000	1.1980
Muscle	89	29 000	17 500	1.6571
Whole body (WB)	23	70 000	58 000	1.2069

and female gonads is such that no such modification is necessary.

Respiratory tract dose

The dose to each of the following respiratory tract regions are calculated separately:

- Absorbed dose to the bronchial basal cells, D (BBbas)
- Absorbed dose to the bronchial secretory cells, D (BBsec)
- Absorbed dose to the bronchiolar region, D(bb)
- Absorbed dose to the alveolar region, D(AI)

where a single quantity is required to represent lung dose, D(lung), then the definition of equivalent dose from ICRP Publication 66 will be used with two modifications:

- Exclude the dose to the thoracic lymph nodes
- Exclude the assumed radiation weighting factor of 20 for alpha particles.

Thus the weighted absorbed dose to the lung, D (lung), is defined as:

$$D(\text{lung}) = 0.333[D(BB_{bas})/\,2 + D(BB_{sec})/2] + 0.333D(\text{bb}) + 0.333D(\text{AI}). \quad (14)$$

A full justification for weighting the absorbed doses in different lung regions in this way is presented by Birchall *et al.*[42] in this issue. A description of the actual results of the dose calculations and a comparison with previous calculations has been published by Vostrotin *et al.*[43].

SUPPLEMENTARY MATERIAL

Supplementary material are available at *Radiation Protection Dosimetry* online.

ACKNOWLEDGEMENTS

We acknowledge the valuable support and assistance of Barrett Fountos, Program Manager, U.S. DOE's Office of Domestic and International Health Studies (AU-13) and of Sergey Romanov, Director of the Southern Urals Biophysics Institute. We also acknowledge the valuable scientific input, help given, and stimulating discussions with D Gregoratto and J W Marsh from Public Health England (PHE).

FUNDING

This work was conducted as part of the Joint Coordinating Committee for Radiation Effects Research (JCCRER) Project 2.4, Mayak Worker Dosimetry. It was jointly funded by the U.S. Department of Energy (U.S. DOE) and the Federal Medical Biological Agency (FMBA) of the Russian Federation.

REFERENCES

1. Puncher, M. and Birchall, A. *A Monte Carlo method for calculating Bayesian uncertainties in internal dosimetry*. Radiat. Prot. Dosim. **132**(1), 1–12 (2008).

2. Puncher, M., Birchall, A. and Bull, R. K. *A method for calculating Bayesian uncertainties on internal doses resulting from complex occupational exposures*. Radiat. Prot. Dosi. **151**(2), 224–236 (2012).
3. Birchall, A. and Puncher, M. *The Mayak Worker Dosimetry System (MWDS-2013): how to reduce hyper-realizations to realizations*. Radiat. Prot. Dosi. **176**(1-2), 154–162 (2017).
4. Birchall, A., Marsh, J. W., Davis, K., Bailey, M. R., Jarvis, N. S., Peach, A. D., Puncher, M., Dorrian, D. and James, A. C. Using IMBA Professional Plus to Estimate Intakes and Doses. Proceedings of the 7th Society for Radiological Protection International Symposium, 'Change and Continuity in Radiation Protection'. Cardiff, June 12–17, 2005, 43–48 (2005).
5. Birchall, A., Puncher, M., Marsh, J. W., Davis, K., Bailey, M. R., Jarvis, N. S., Peach, A. D., Dorrian, M.-D. and James, A. C. 'IMBA PROFESSIONAL PLUS: A Flexible Approach to Internal Dosimetry.' Presented at IM2005 European Workshop on Individual Monitoring of Ionising Radiation. Vienna, Austria, April 11–15 (2005).
6. Birchall, A., Puncher, M., Marsh, J. W., Davis, K., Bailey, M. R., Jarvis, N. S., Peach, A. D., Dorrian, M. D. and James, A. C. *IMBA professional plus: a flexible approach to internal dosimetry*. Radiat. Prot. Dosi. **125** (1–4), 194–197 (2007).
7. Dorrian, M.-D., Vostrotin, V., Birchall, A., Zhdanov, A. and Erykalov, A. *The Mayak Worker Dosimetry System (MWDS-2013): quality assurance of organ doses calculation (Phase I)*. Radiat. Prot. Dosimetry. **176**(1-2), 166–181 (2017).
8. Vostrotin, V., Birchall, A., Zhdanov, A. and Puncher, M. *The Mayak Worker Dosimetry System (MWDS-2013): quality assurance of organ doses calculation (Phase II)*. Radiat. Prot. Dosi. **176**(1-2), 182–189 (2017).
9. Birchall, A., Puncher, M. and Vostrotin, V. *The Mayak Worker Dosimetry System (MWDS-2013): treatment of uncertainty in model parameters*. Radiat. Prot. Dosi. **176**(1-2), 144–153 (2017).
10. Vostrotin, V., Birchall, A., Zhdanov, A., Gregoratto, D., Suslova, K., Marsh, J. W. and Efimov, A. *The Mayak Worker Dosimetry System (MWDS-2013): uncertainty in the measurement of Pu activity in a 24-hour urine sample of a typical Mayak PA worker*. Radiat. Prot. Dosimetry. **176**(1-2), 106–116 (2017).
11. ICRP. Basic Anatomical and Physiological Data for Use in Radiological Protection: Reference Values. ICRP Publication 89, International Commission on Radiological Protection (ICRP) (2002).
12. Schadilov, A. Y., Khokhryakov, V. F., Kudryavtseva, T. I. and Vostrotin, V. V. *Влияние пентацина на уровень экскреции плутония из организма человека [Ca-DTPA effects on plutonium excretion from the human organism]*. Bulletin Anthrax Medicine. 2, 128–132 (2005).
13. ANSI N13.30 1996 Performance Criteria for Radiobioassay (McLean, VA: An American National Standard, Health Physics Society) (1996).
14. ISO. Determination of the Characteristic Limits (Decision Threshold, Detection Limit and Limits of the Confidence Interval) for Measurements of Ionizing Radiation—Fundamentals and Application. ISO 11929: 2010. International Organization for Standardization (ISO), Geneva, Switzerland (2010).
15. Sokolova, A. B., Birchall, A., Efimov, A. V., Vostrotin, V. V. and Dorrian, D. *The Mayak Worker Dosimetry System (MWDS-2013): determination of the individual scenario of inhaled plutonium intake in the Mayak workers*. Radiat. Prot. Dosimetry. **176**(1-2), 83–89 (2017).
16. Puncher, M., Birchall, A. and Bull, R. K. *An intake prior for the Bayesian analysis of plutonium and uranium exposures in an epidemiology study*. Radiat. Prot. Dosimetry. **162**(3), 306–315 (2014).
17. ICRP. Occupational Intakes of Radionuclides, Part 1. ICRP Publication 130, International Commission on Radiological Protection (ICRP) (2015).
18. ICRP. Human Respiratory Tract Model for Radiological Protection. ICRP Publication 66; Ann ICRP 24(1–3), International Commission on Radiological Protection (ICRP) (1994).
19. Smith, J. R. H., Birchall, A., Etherington, G., Ishigure, N. and Bailey, M. R. *A revised model for the deposition and clearance of inhaled particles in human extra-thoracic airways*. Radiat. Prot. Dosi. **158**(2), 135–147 (2014).
20. Puncher, M., Birchall, A. and Bull, R. K. *Uncertainties on lung doses from inhaled plutonium*. Radiat. Res. **176** (4), 494–507 (2011).
21. Falk, R., Philipson, K., Svartengren, M., Jarvis, N., Bailey, M. and Camner, P. *Clearance of particles from small ciliated airways*. Exp. Lung Res. **23**(6), 495–515 (1997).
22. Falk, R., Philipson, K., Svartengren, M., Bergmann, R., Hofmann, W., Jarvis, N., Bailey, M. and Camner, P. *Assessment of long-term bronchiolar clearance of particles from measurements of lung retention and theoretical estimates of regional deposition*. Exp. Lung Res. **25** (6), 495–516 (1999).
23. Gregoratto, D., Bailey, M. R. and Marsh, J. W. *Modelling particle retention in the alveolar–interstitial region of the human lungs*. J. Radiol. Protect. **30**(3), 491–512 (2010).
24. Davesne, E., Paquet, F., Ansoborlo, E. and Blanchardon, E. *Absorption of plutonium compounds in the respiratory tract*. J. Radiol. Protect. **30**(1), 5–21 (2010).
25. James, A. C., Sasser, L. B., Stuit, D. B., Glover, S. E. and Carbaugh, E. H. *USTUR whole body case 0269: demonstrating effectiveness of iv ca-DTPA for Pu*. Radiat. Prot. Dosi. **127**, 449–455 (2007).
26. Birchall, A., Puncher, M., Harrison, J., Riddell, A., Bailey, M. R., Khokryakov, V. and Romanov, S. *Plutonium worker dosimetry*. Radiat. Environ. Biophys. **49**(2), 203–212 (2010).
27. Puncher, M., Pellow, P. G. D., Hodgson, A., Etherington, G. and Birchall, A. *The Mayak Worker Dosimetry System (MWDS-2013): a Bayesian analysis to quantify pulmonary binding of plutonium in lungs using historic beagle dog data*. Radiat. Prot. Dosi. **176** (1-2), 32–44 (2017).
28. Tolmachev, S. Y., Nielsen, C. E., Avtandilashvili, M., Puncher, M., Martinez, F., Thomas, E. M., Miller, F. L., Morgan, W. F. and Birchall, A. *The Mayak Worker Dosimetry System (MWDS 2013): soluble plutonium distribution in the lungs of an occupationally exposed worker*. Radiat. Prot. Dosimetry. **176**(1-2), 45–49 (2017).
29. Puncher, M., Birchall, A. and Tolmachev, S. Y. *The Mayak Worker Dosimetry System (MWDS 2013): a*

re-analysis of USTUR Case 0269 to determine whether plutonium binds to the lungs. Radiat. Prot. Dosimetry. **176**(1-2), 50–61 (2017).
30. Puncher, M., Birchall, A., Sokolov, M. A. and Suslova, K. G. *The Mayak Worker Dosimetry System (MWDS-2013): plutonium binding in the lungs—an analysis of Mayak workers*. Radiat. Prot. Dosimetry. **176**(1-2), 62–70 (2017).
31. Gilks, W. R., Richardson, S. and Spiegelhalter, D. J. Introducing Markov Chain Monte Carlo. In: In Markov Chain Monte Carlo in Practice (London: Chapman and Hall) (1996).
32. Suslova, K. G., Orlova, I. A., Burikova, E. A., Sokolova, A. B., Salamatova, V. Y., Tolmachev, S. Y. and Miller, S. C. *The Mayak Worker Dosimetry System-2013: estimation of plutonium skeletal content from limited autopsy bone samples from Mayak PA workers*. Radiat. Prot. Dosi. **176**(1-2), 117–131 (2017).
33. Sokolova, A. B. and Suslova, K. G. *The Mayak Worker Dosimetry System (MWDS-2013): estimate of Pu content in lungs and thoracic lymph nodes from limited autopsy samples*. Radiat. Prot. Dosi. **176**(1-2), 132–143 (2017).
34. Puncher, M., Birchall, A., Suslova, K. G. and Sokolova, A. B. *The Mayak Worker Dosimetry System (MWDS 2013): determination of lung solubility of plutonium in Mayak workers*. Radiat. Prot. Dosi. (2016) (This issue).
35. Etherington, G., Stradling, G. N., Hodgson, A. and Fifield, L. K. *Anomalously high excretion of Pu in urine following inhalation of plutonium nitrate*. Radiat. Prot. Dosi. **105**, 321–324 (2003).
36. ICRP. Limits for Intakes of Radionuclides by Workers. ICRP Publication 30; Ann ICRP 2(3-4), International Commission on Radiological Protection (ICRP) (1979).
37. Leggett, R. W., Eckerman, K. F., Khokhryakov, V. F., Suslova, K. G., Krahenbuhl, M. P. and Miller, S. C. *Mayak worker study: an improved biokinetic model for reconstructing doses from internally deposited plutonium*. Radiat. Res. **164**(2), 111–122 (2005).
38. Birchall, A., Dorrian, M. D., Suslova, K. G. and Sokolova, A. B. *The Mayak Worker Dosimetry System (MWDS-2013): a comparison of intakes based on urine and autopsy data from Mayak workers using the Leggett systemic model for plutonium*. Radiat. Prot. Dosimetry. **176**(1-2), 90–94 (2017).
39. Puncher, M. and Harrison, J. D. *Uncertainty analysis of doses from ingestion of plutonium and americium*. Radiat. Prot. Dosi. **148**(3), 284–296 (2012).
40. ICRP. Dose Coefficients for Intakes of Radionuclides by Workers. ICRP Publication 68; Ann ICRP 24(4), International Commission on Radiological Protection (ICRP) (1994).
41. Birchall, A. and Sokolova, A. B. *The Mayak Worker Dosimetry System (MWDS-2013: treatment of organ masses in the calculation of organ doses*. Radiat. Prot. Dosi. **176**(1-2), 102–105 (2017).
42. Birchall, A. and Marsh, J. W. *The Mayak Worker Dosimetry System (MWDS-2013): how to weight the absorbed dose to different lung regions in the calculation of lung dose*. Radiat. Prot. Dosi. **176**(1-2), 95–101 (2017).
43. Vostrotin, V., Birchall, A., Zhdanov, A., Puncher, M., Efimov, A., Napier, B., Sokolova, A., Miller, S. and Suslova., K. *The Mayak Worker Dosimetry System (MWDS-2013): internal dosimetry results*. Radiat. Prot. Dosi. **176**(1-2), 190–201 (2017).